

# Numerical Simulations of Ideal Chain Model of Polymer using the Freely Jointed Chain (FJC)

Nguyen Truong Phong & Moreno Sarria Cindy Catalina

## 1 Introduction

Polymers, also known as macro-molecules, are built up of a large number of molecular units that are linked together by covalent bonds. Polymers are widely used advanced materials that can be found almost anywhere in our daily lives. The physics of polymers studies the physical properties and behavior of polymer materials.<sup>2</sup>

In the study of polymer physics, discrete models describe the behavior of polymer chains at the molecular level. These models simplify the complex interactions within polymers, making it easier to analyze their properties.

The Freely-jointed chain (FJC) model assumes that each monomer in the chain is connected by a freely rotating joint, and the segments between joints are of fixed length.<sup>1</sup> The Freely Jointed Chain (FJC) model is commonly used to calculate statistical parameters such as the mean square end-to-end distance of a polymer chain  $\langle Q^2 \rangle$ , which provides information about its size and shape. The model also makes it easier to calculate other properties, such as the chain's radius of gyration  $R_g$ , which provides information about the average size of the polymer chain.

Comparing these model-derived predictions to experimental measurements, particularly the gyration radius, allows us to evaluate the model's accuracy. In this project, we employ the FJC model for the simulation of polymer chains, calculate parameters  $\langle Q^2 \rangle$ , radius of gyration  $R_g$  and compare the result with theory. Probability distribution of  $Q$  and the Guiner approximation will also be considered. Then we extend the polymer in a given direction by applying a force  $\mathbf{F}$  and compute the force-extension curve using a Metropolis Monte-Carlo algorithm

## 2 Methods

A simple simulation of the FJC model was developed, producing randomly  $N$  normalized vectors representing a configuration of a  $N+1$  atoms polymer. The bounds of the chain of atoms had a constant length of  $b_l = 3$  such as in fig. 1. Generating several amount of configurations, the simulation computes the mean square end-to-end distance  $\langle Q^2 \rangle$ , which in the FJC model is given by,

$$\langle Q^2 \rangle = Nb^2 + b^2 \sum_{i \neq j} \langle \cos \theta \rangle_{ij} = Nb^2, \quad (1)$$

since  $\langle \cos \theta \rangle_{ij} = 0$  in this model. Using the grate amount of configurations, the probability distribution of the end-to-end distance  $P(Q)$  plotted in a histogram and compared with the theory prediction,

$$P(Q) = 4\pi Q^2 \left( \frac{3}{2\pi Nb^2} \right)^{3/2} \exp \left( -\frac{3Q^2}{2Nb^2} \right), \quad (2)$$

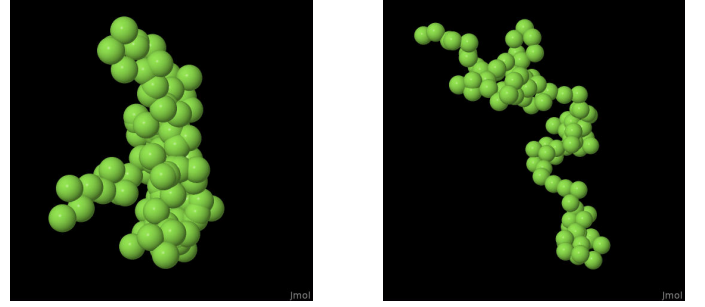


**Fig. 1** Two polymer structures generated from FJC model simulations for  $N = 100$  and  $b = 3.0$ .

The mean square radius of gyration,

$$\langle R_g^2 \rangle = \frac{1}{N} \sum_{i=0}^N (\vec{R}_i - \vec{R}_{cm})^2, \quad (3)$$

was also computed, as well as its convergence to  $\frac{Nb^2}{6}$  when  $N \rightarrow \infty$ . For all of these variables, an analysis on the influence of the number of configurations were performed on the variables above in order to appreciate the behaviour of the error comparing with the theory value.

Then, fixing the number of molecules to  $N = 100$ , the structure factor  $I(k)$  was computed and compared with the Guiner approximation,

$$I(k) = (N+1)^2 \left[ 1 - \frac{(kR_g)^2}{3} \right]. \quad (4)$$

Using the structure factor, a value of the mean square radius of gyration  $\langle R_g^2 \rangle$  was extracted and compared with the theoretical value already computed.

Finally, a force  $F$  in the  $x$  axis was considered in the simulation. A random initial configuration was computed, and then applying the Metropolis Monte-Carlo algorithm, the evolution of time of the molecule was simulated. Considering the potential as  $V = -\vec{F} \cdot \vec{Q}$ , each move was accepted (rejected) if a random value between 0 to 1 is lesser (greater) than  $\exp(-\Delta V)$ . Using a fix force value,  $F = 20$  (arbitrary units), the evolution of the length in the  $x$  axis was computed. Then using a range of forces, from 0 to 10, the fraction of the maximum length reach was related with the force applied, which would behave as,

$$|\vec{Q} \cdot \vec{u}_x| = Nb \left[ \coth(\alpha) - \frac{1}{\alpha} \right], \quad (5)$$

with  $\alpha = \frac{Fb}{k_B T}$ .

## 3 Results and Discussion

The plots below shows the comparison of mean square end-to-end distance  $\langle Q^2 \rangle$  and the mean square radius gyration  $\langle R_g^2 \rangle$  between

simulation and theory where bond length  $b = 3.00$ .

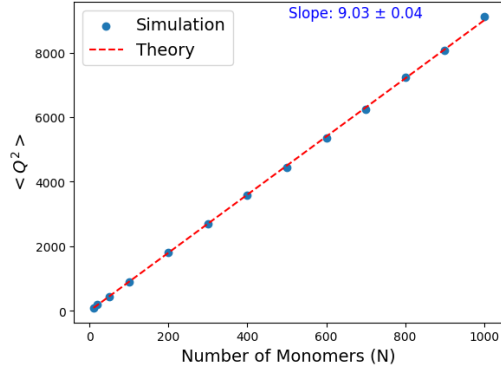


**Fig. 2** Comparison of  $\langle Q^2 \rangle$  between simulation and theory for  $10^4$  conformations simulation

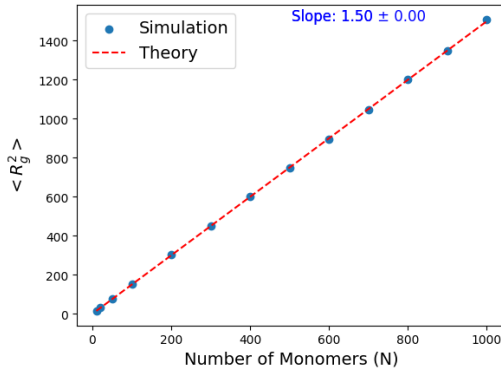


**Fig. 3** Comparison of  $\langle R_g^2 \rangle$  between simulation and theory for  $10^4$  conformations simulation

Obviously we see the linear relation  $\langle Q^2 \rangle = 9.03N$ , agrees with the theory where  $\langle Q^2 \rangle = 9N$ . The same result was achieved with the mean square radius gyration  $\langle R_g^2 \rangle = 1.5N$ , strongly align with the theory where  $\langle R_g^2 \rangle = 1.5N$ .

Influence of the number of conformations  $T$  is displayed in table 1. We calculate the difference to the theory  $\Delta\langle Q^2 \rangle$  and  $\Delta\langle R_g^2 \rangle$  by the formula

$$\Delta\langle Q^2 \rangle = (\langle Q^2 \rangle - \langle Q_{th}^2 \rangle) / \langle Q_{th}^2 \rangle * 100\% \quad (6)$$

$$\Delta\langle R_g^2 \rangle = (\langle R_g^2 \rangle - \langle R_{th}^2 \rangle) / \langle R_{th}^2 \rangle * 100\% \quad (7)$$

T	$\Delta\langle Q^2 \rangle, \%$	$\Delta\langle R_g^2 \rangle, \%$
10	15.68	6.35
$10^2$	14.93	7.11
$10^3$	3.67	1.82
$10^4$	0.70	1.41
$10^5$	0.13	1.01

**Table 1** Influence of  $T$  to the simulation result

When the number of conformations  $T$  is below  $10^3$ , there are high variance of  $\Delta\langle Q^2 \rangle$  and  $\Delta\langle R_g^2 \rangle$  with the theory. The differences with theory decrease significantly when  $T > 10^3$ .

Now we consider the probability distribution of the end-to-end distance  $P(Q)$  for  $N=100$  with  $10^4$  conformations. The shape of the distribution is a Gaussian-shaped curve, which agrees with the equation (2). In the case when  $N=2$ , the linear relation  $P(Q) = Q/2b^2$  was observed. The simulation results in both case are align with the theory.

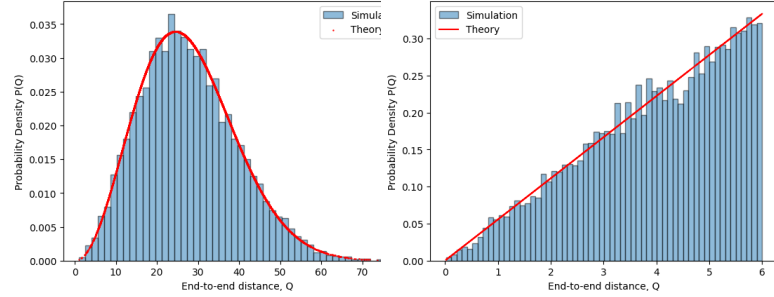


**Fig. 4** Probability distribution  $P(Q)$  and comparison with theory when  $N=100$  (left) and  $N=2$  (right) with  $10^4$  conformations.

The Intensity of the scattering  $I(k)$  simulated was compared with the Guinier approximation given by equation (4) as shown in the graph below. The result was normalized with the factor of  $(N+1)^2$ . We can observe that when  $k$  is small, Guinier approximation is close to the simulated  $I(k)$  data.

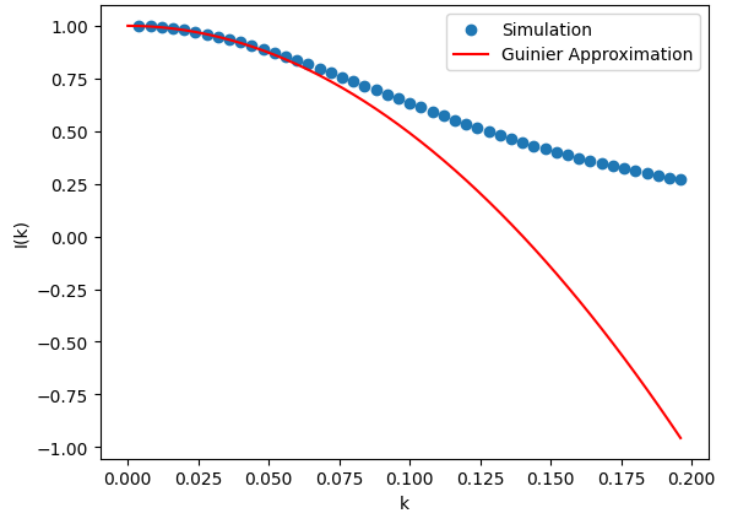


**Fig. 5** The comparison of Intensity of scattering  $I(k)$  between simulation and the Guinier approximation for  $10^3$  conformations and  $N=100$

Consider the case when  $k < 0.04$ , we solve the linear regression of  $I(k)$  and  $k^2$  and found the value of  $R_g^2 = 147.35$ , which is close to the value  $\langle R_g^2 \rangle = 151.52$ . The linear relation is observable in the graph of  $I(k^2)$  when  $k < 0.04$ .

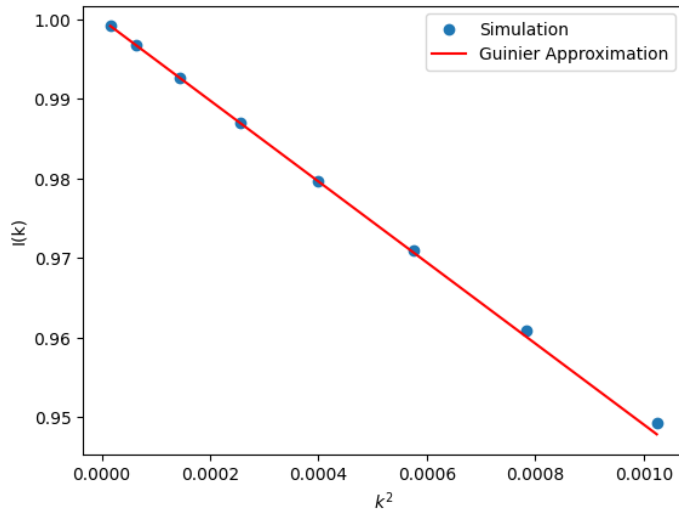


**Fig. 6** Linear relation with  $k < 0.04$  of the intensity of scattering  $I(k^2)$  between simulation and the Guinier approximation for  $10^3$  conformations and  $N=100$

Finally, the following plots show the results of the Montecarlo simulation. The fig. 7 illustrates the  $Q_x$  value of the simulated polymer in function of time when a force on the  $x$  axis was applied. We can appreciate how for greater values of  $t$ ,  $Q_x$  approaches asymptotically to the max value, this being  $Nb$ . In the case of the fig. 8, the relation between the force applied and the extension percentage (meaning  $Q_x/Nb$ ) is shown, having a strong relation with eq. (5), which is expected.

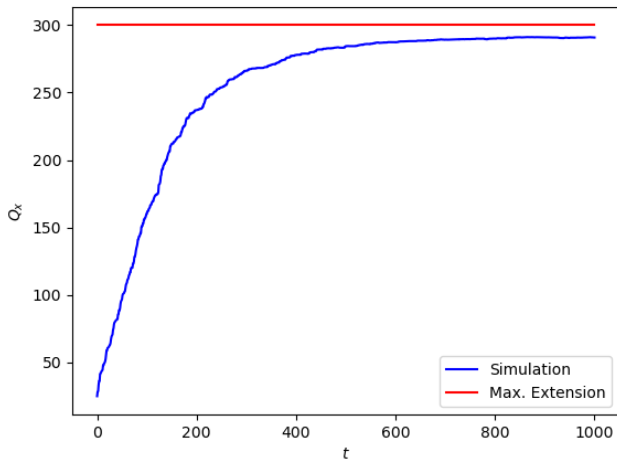


**Fig. 7** Extension on the  $x$  axis reached by the polymer in function of the time applying a Force in the  $x$  axis.

## 4 Conclusion

In this report, we simulated different polymer chains based on the Freely-Jointed Chain model and achieved the results that strongly align with theoretical predictions.

The agreement observed in mean square end-to-end distance, radius of gyration, where we observed a linear relation between

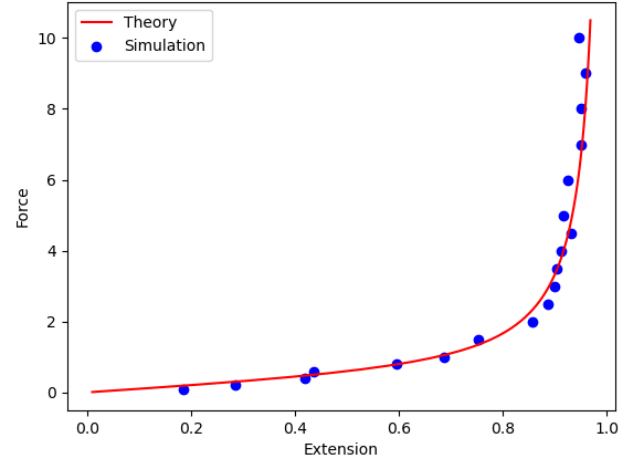


**Fig. 8** Maximum percentage of Extension on the  $x$  axis reached by the polymer in function of the Force applied.

number of monomers  $N$  and  $\langle Q^2 \rangle$  and  $\langle R_g^2 \rangle$ . We also observed the Gaussian-shaped probability distribution  $P(Q)$  when  $N=100$  and a linear distribution  $P(Q)$  when  $N=2$ . The structure factor also showed strong agreement with the theory.

Metropolis Monte-Carlo simulation algorithm was also used in the stretching experiment of the polymers. A force exerted in one direction can stretch the polymer, and the polymer can be stretched to the nearly maximal length  $Nb$  in our simulation. Also, the relation between extension ratio and the applied force was studied and strongly agreed with the theory. Increase in the applied force leads to the increment of the extension ratio.

Our analysis supports the validity of the Freely-Jointed Chain model in capturing essential aspects of polymer behavior. The successful alignment of our simulation results with theoretical expectations demonstrates the model's accuracy and reliability in describing polymer dynamics. While this study provides valuable insights, it also opens avenues for further exploration, considering the limitations and potential areas for future research.

## 5 References

### Notes and references

- 1 Michael R. Buche, Meredith N. Silberstein, and Scott J. Grutzik. Freely jointed chain models with extensible links. *Phys. Rev. E*, 106:024502, Aug 2022.
- 2 Hassan Namazi. Polymers in our daily life. *BioImpacts*, 7:73–74, 06 2017.